Progress in Natural Science: Materials International 2013;23(5):514–518

Chinese Materials Research Society

Progress in Natural Science: Materials International

www.elsevier.com/locate/pnsmi
www.sciencedirect.com

LETTERS

Hybrid solar cells based on poly(3-hexylthiophene) and electrospun TiO_2 nanofibers modified with CdS nanoparticles

Shingchung Lo, Zhike Liu, Jinhua Li, Helen Laiwa Chan, Feng Yan*

Department of Applied Physics and Materials Research Centre, The Hong Kong Polytechnic University, Hong Kong, China

Received 8 February 2013; accepted 20 July 2013
Available online 25 October 2013

KEYWORDS

Organic solar cells;
TiO_2 nanofiber;
CdS nanoparticle;
Surface modification

Abstract Organic–inorganic hybrid solar cells based on poly(3-hexylthiophene) and electrospun TiO_2 nanofibers were fabricated by solution process. The efficiency of the device was improved by modifying CdS nanoparticles on the surface of TiO_2 by electrochemical method. The CdS layer can lead to the increase of both open circuit voltage and short circuit current of the device, which are attributed to enhanced exciton dissociation and light absorption and suppressed carrier recombination by CdS at the heterojunction. However, too thick CdS layer led to increased series resistance and decreased efficiency of the device. Therefore, the optimum condition of the CdS deposition was obtained, which increased the power conversion efficiency of the device for about 50%. Our results indicate that the surface modification on the inorganic semiconductor layer is an effect way to improve the performance of the hybrid solar cells.

1. Introduction

Photovoltaic technology is the key strategy to alleviate the energy crisis in the world. However, commercial silicon solar cells are too expensive to be used as the main energy source for our normal life. Therefore, third-generation solar cells based on functional materials have been developed recently with a view to realizing efficient and low-cost photovoltaic devices. Devices composed of organic materials, such as conjugated polymers and small molecule organic semiconductors [1–9], have received much research interest because of the following advantages, including low cost, easy fabrication, flexibility and potential of large area production [2].

Recently, organic solar cells based on conjugated polymer-fullerene composites with the power conversion efficiencies (PCE) up to 9% under AM1.5 solar light illumination have been achieved [9]. However, low carrier mobilities and poor stability of the active layers hinder the practical applications of the devices [3–5]. Many researchers attempted to overcome this problem by replacing the organic electron transporter with inorganic semiconductors [10–15], such as CdSe, TiO_2 and ZnO, because the n-type semiconductors

*Corresponding author.
E-mail address: apafyan@polyu.edu.hk (F. Yan).

Peer review under responsibility of Chinese Materials Research Society.

Production and hosting by Elsevier

1002-0071 © 2013 Chinese Materials Research Society. Production and hosting by Elsevier B.V. All rights reserved.
http://dx.doi.org/10.1016/j.pnsc.2013.09.003

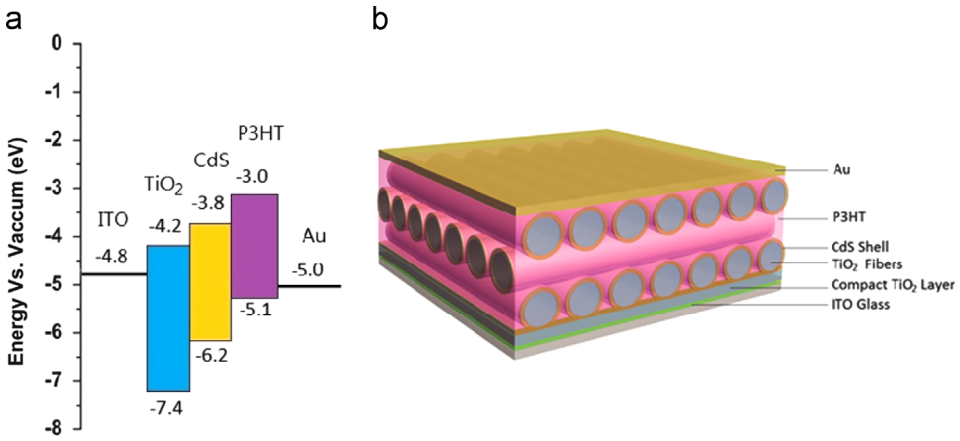

Fig. 1 (a) Energy band structure of the hybrid solar cell based on P3HT and TiO_2 nanofibers modified with CdS. (b) Device structure of the hybrid solar cell based on P3HT and cross-aligned TiO_2 nanofibers modified with CdS.

exhibit more stable physical and chemical properties. Furthermore, those semiconductors possess several advantages over their organic counterparts, including high electron mobility, high dielectric constant and facile control of the size and the shape of nanostructure. Therefore, inorganic nanoparticles [15], nanorods [14,16–19], nanofibers [12,13,20,21] and porous films [11,22] have been popularly used in hybrid solar cells. Various techniques have been employed to improve the interfacial area and the properties of the organic–inorganic heterojunctions [13,22]. Although the PCEs of hybrid solar cells still lag behind those of the whole organic ones, higher PCEs would be expected in the future when the device physics is further understood and new breakthroughs in synthesis of materials and device fabrication are achieved.

In this paper, photovoltaic devices composed of TiO_2 nanofibers, CdS interfacial layer and poly(3-hexylthiophene) (P3HT) have been studied. TiO_2 nanofibers were prepared by electrospinning process [23,24], which is a convenient technique to fabricate fibers with high aspect ratio and nanoscale diameter. The size and the alignment of the nanofibers have been controlled by choosing suitable solvent and processing conditions. CdS layer was deposited on TiO_2 nanofibers by facile solution process [25–28]. As shown in Fig. 1, CdS is the interfacial layer between TiO_2 and P3HT, which can enhance exciton dissociation, prevent the carrier recombination and increase the open circuit voltage of the devices because of the cascaded band structure of the multilayer film [13,29]. The performance improvement induced by modifying CdS on TiO_2 surface was consistent with the results reported in literature [30].

2. Experimental

The hybrid solar cells were fabricated on patterned ITO glass substrates (sheet resistance: ~15 Ω/sq) with the structure shown in Fig. 1. Before device fabrication, ITO substrates were cleaned in an ultrasonic bath using ethanol, acetone and isopropyl alcohol (IPA). Oxygen plasma cleaning was subsequently applied to remove organic remnant. A sol–gel solution of 0.25 M titanium (IV) n-butoxide in ethanol was spin-coated at 6000 rpm for 30 s on the cleaned ITO glass and then annealed at 500 °C for 2 min by rapid thermal process to make a compact and crystallized TiO_2 thin layer of about 40 nm thick. This layer can serve as a hole-blocking layer and improve the adhesion of electrospun fibers in next step.

High-molecular-weight poly(vinylpyrrolidone) (PVP) (M_W = 1,300,000 g/mol) was chosen to dissolve in 2-Methoxyethanol (EGME) with titanium (IV) tetra iso-propoxide (TTIP) to be a sol-gel precursor to titania [24]. A well-mixed solution composed of PVP (0.05 g/ml), TTIP (0.05 g/ml), EGME (0.73 g/ml), IPA (0.23 g/ml), acetic acid (0.01 g/ml) and acetylacetone (0.01 g/ml) was electrospun at a feeding rate of about 0.1 ml/h under 40 kV/m electric field strength. The substrate was stuck on a rotating collector to obtain better alignment of nanofibers since the ordered nanofibers are more favorable for obtaining higher PCEs in the hybrid solar cells [13,23]. Each layer was collected for 30 min with the alignment direction perpendicular to adjacent ones. Three layers of TiO_2 nanofibers were collected to form fibrous films followed by rapid thermal process at 500 °C for 10 min to remove organic compound and crystallize TiO_2 nanofibers [13].

CdS nanoparticles were deposited on the fibrous films by electrochemical deposition in 0.05 M CdS water solution [31], which was prepared by mixing the same volume of 0.1 M cadmium nitrate ($Cd(NO_3)_2$) solution and 0.1 M thioacetamide (C_2H_5NS) solution. CdS particles are formed in the solution according to the following reaction:

$$Cd^{2+} + CH_3CSNH_2 + H_2O \rightarrow CdS + CH_3CONH_2 + 2H^+$$

A platinum plate and an Ag/AgCl (sat. KCl) electrode were used as the counter electrode and the reference electrode, respectively [30]. In order to obtain uniform deposition on the fibrous layer, small negative constant current ($\sim 10^{-4}$ A) was applied to the ITO substrate and the whole process was performed under room temperature. The deposition amounts of nanoparticles were controlled by the treatment time. The fibrous films were rinsed for several times by deionized water to remove physisorbed particles.

P3HT solution (Reike, regioregularity is ~93%, 30 mg/ml in toluene) was prepared and spin-coated on the fibrous films at 1500 rpm for 30 s. The coated samples were immediately transferred to a glovebox filled with high purity nitrogen and annealed at 100 °C for 20 min to remove solvent, oxygen and moisture, and enhance the crystallinity of the P3HT film. Then, a gold top electrode of about 80 nm thick was deposited on the P3HT layer by thermal evaporation.

The current density–voltage (J–V) performance of the solar cells was characterized by Keithley 2400 source meter under 100 mW/cm^2 illumination generated by Newport 91160 (300 W) solar simulator with an AM1.5G filter. The intensity was calibrated by a standard silicon solar cell [4]. The UV–visible light absorption

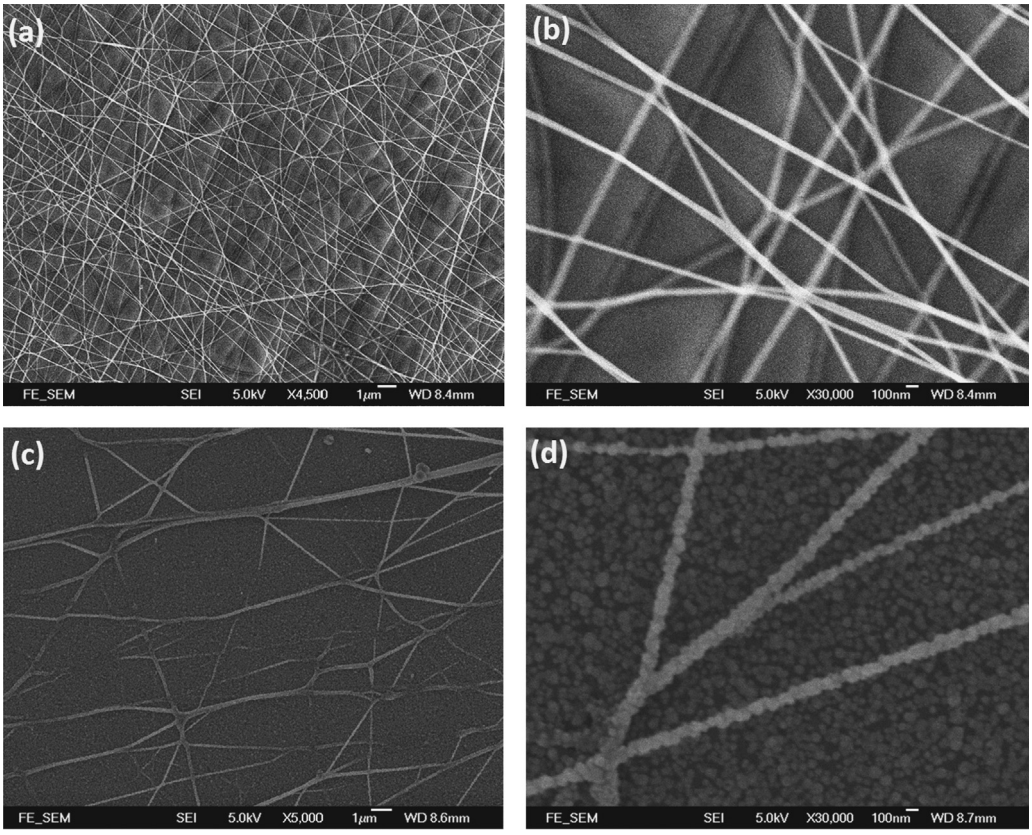

Fig. 2 (a) (b) SEM images of electrospun TiO_2 nanofibers; (c) (d) SEM images of electrospun TiO_2 nanofibers modified with CdS layer.

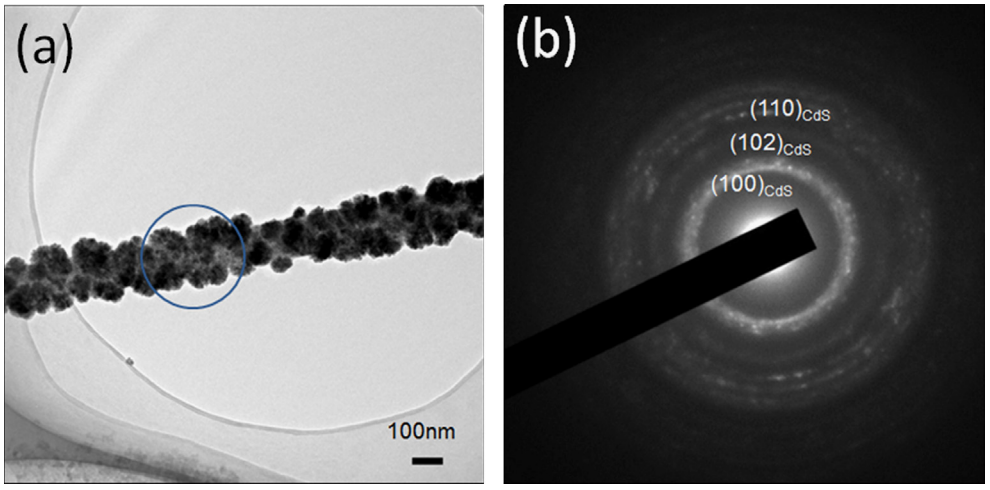

Fig. 3 (a) TEM image and (b) deflection pattern of an electrospun TiO_2 nanofiber modified with CdS particles.

spectra of materials were measured by Shimadzu UV-2550 UV–vis spectrophotometer [32]. The dimension, morphology and crystallinity of TiO_2 nanofibers were studied by scanning electron microscopy (SEM, Quanta 299 FEG system, FEI Co., U.S.A.) and transmission electron microscopy (TEM, JEOL 2010, Japan).

3. Results and discussion

Fig. 2a and b show the morphology of the electrospun TiO_2 nanofibers observed under scanning electron microscopy (SEM). The nanofibers are cross-aligned and have diameters ranged between 30 nm to 100 nm. Fig. 2c and d show the SEM images of the TiO_2 nanofibers with CdS modification by electrochemical deposition process [31]. The images reveal that many CdS nanoparticles were attached on the surface of the TiO_2 nanofibers. Fig. 3a shows the image of the CdS modified TiO_2 nanofibers under transmission electron microscopy (TEM). The CdS nanoparticles attached on the TiO_2 surface and fibers have the sizes ranged from 20 nm to 100 nm. The hexagonal structure of CdS can be verified by the electron diffraction pattern under TEM, as shown in Fig. 3b.

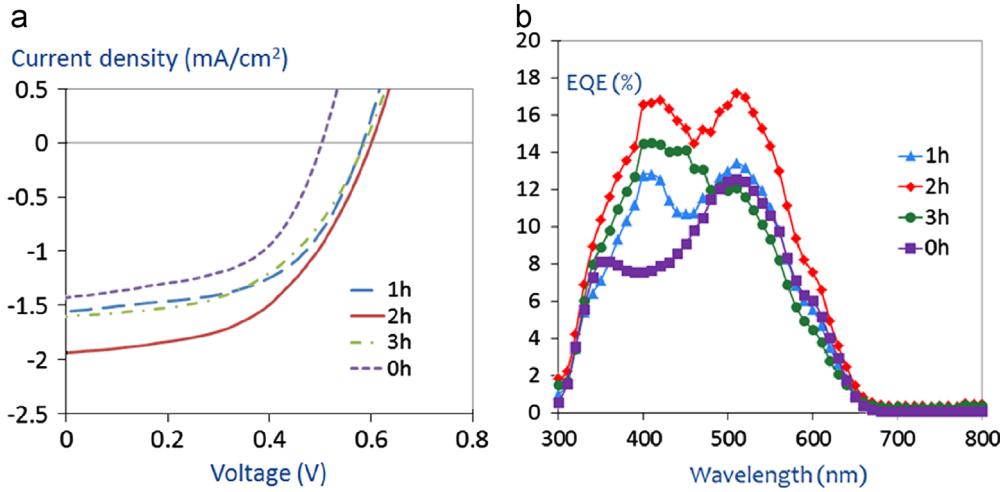

Fig. 4 (a) *J–V* characteristics and (b) external quantum efficiency (EQE) of the hybrid solar cells based on TiO_2/P3HT or TiO_2/CdS/P3HT with different CdS deposition time.

Table 1 Photovoltaic parameters of hybrid solar cells fabricated with different CdS deposition time.

Deposition time of CdS (h)	Voc (V)	Jsc (mA/cm^2)	FF	PCE (%)
0	0.505	1.43	0.54	0.39
1	0.584	1.56	0.55	0.50
2	0.601	1.93	0.52	0.60
3	0.588	1.60	0.51	0.48

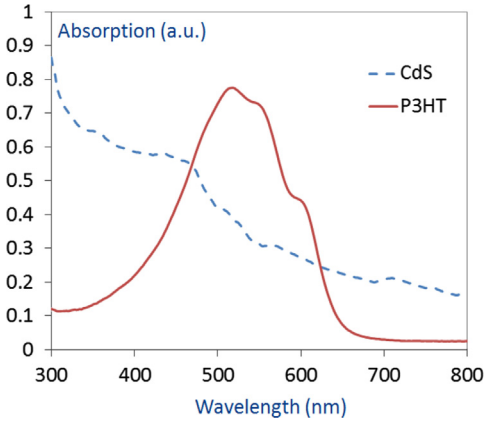

Fig. 5 Absorption spectra of P3HT and CdS layers.

The *J–V* characteristics of the hybrid solar cells with different deposition time of CdS were characterized under AM1.5 solar simulator and shown in Fig. 4a. The CdS-modified devices exhibit higher open-circuit voltages than that of the unmodified one, which can be attributed to the longer lifetime of carriers in the devices since the CdS layers prohibit the recombination of electrons and holes [13]. Furthermore, higher short circuit current can be observed in the devices with CdS modification. The optimum deposition time of CdS was about 2 hr and improved the PCE from 0.39% to 0.60%. As the fill factors (FF) of devices were similar, the higher efficiency should be attributed to the increase of both the open-circuit voltage and the short-circuit current. However, as shown in Fig. 4a, too thick CdS layer would not be beneficial to the device performance because of the limited diffusion length of charge carriers in CdS. The photovoltaic parameters of all devices are summarized in Table I. It is notable that the series resistances of the solar cells calculated from the slope of the *J–V* characteristic have the lowest value in the unmodified device and increase with the increase of the CdS deposition time. Therefore, the decrease of device efficiency at long deposition time (> 3 hr) is due to the high resistance of the CdS layer.

Fig. 4b shows the external quantum efficiencies (EQE) of the devices, which exhibit the contribution of current from illumination at different wavelengths. For normal TiO_2/P3HT device, a broad peak about 520 nm indicates the photocurrent produced by P3HT and a small peak about 350 nm belongs to TiO_2 nanofibers for the large band gap of TiO_2. The contribution of P3HT can be verified by the strong absorption of P3HT peaked at 520 nm and absorption shoulder at 600 nm showed in Fig. 5 [32]. For the TiO_2/CdS/P3HT devices, one more peak at 400 nm represents the photocurrent induced by CdS nanoparticle, as reported by Spoerke et al. [29]. Meanwhile, the photocurrent of the device increases with the increase of deposition time (0 to 2 hr). Therefore, it is reasonable to conclude that CdS interfacial layer benefits to light absorption and charge separation, and prevents the recombination of charge carriers at the heterojunction. If the deposition time is too long (3 hr) and the CdS layer is too thick, the EQE of the device is suppressed for the higher series resistance induced by CdS layer as explained above.

4. Conclusion

In conclusion, hybrid solar cells based on electrospun n-type TiO_2 nanofibers and p-type conjugated polymer P3HT have been fabricated by facile solution process. The device performance was improved by modifying the TiO_2 nanofibers with CdS nanoparticles deposited by electrochemical method. The PCE of the device was dramatically increased after the CdS modification because of the increased short circuit current and open circuit voltage. According to the band structure of the TiO_2/CdS/P3HT multilayer film, the CdS layer can enhance exciton dissociation and prohibit carrier recombination at the heterojunction, and can

absorb light at the wavelength around 400 nm. All of these effects can lead to a higher short circuit current and a higher open circuit voltage of the device. However, too thick CdS layer is not favorable for the device performance because of the increased series resistance of the device. Therefore, the optimum amount of CdS modification was achieved by electrochemical deposition for about 2 h and resulted in ~50% increase in the PCE of the device.

Acknowledgment

This work is financially supported by the Research Grants Council (RGC) of Hong Kong, China (project number: PolyU5322/10E) and the Hong Kong Polytechnic University (project number: A-PK07).

References

[1] W.J.E. Beek, M.M. Wienk, R.A.J. Janssen, Advanced Materials 16 (2004) 1009–1013.
[2] G. Li, V. Shrotriya, J. Huang, Y. Yao, T. Moriarty, K. Emery, Y. Yang, Nature Materials 4 (2005) 864–868.
[3] M. Campoy-Quiles, T. Ferenczi, T. Agostinelli, P.G. Etchegoin, Y. Kim, T.D. Anthopoulos, P.N. Stavrinou, D.D.C. Bradley, J. Nelson, Nature Materials 7 (2008) 158–164.
[4] S.J. Wu, J.H. Li, Q.D. Tai, F. Yan, Journal of Physical Chemistry C 114 (2010) 21873–21877.
[5] Q.D. Tai, J.H. Li, Z.K. Liu, Z.H. Sun, X.Z. Zhao, F. Yan, Journal of Materials Chemistry 21 (2011) 6848–6853.
[6] Y.Y. Liang, Z. Xu, J.B. Xia, S.T. Tsai, Y. Wu, G. Li, C. Ray, L.P. Yu, Advanced Materials 22 (2010) E135–E138.
[7] Z.K. Liu, J.H. Li, F. Yan, Advanced Materials 25 (2013) 4296–4301.
[8] Z.K. Liu, J.H. Li, Z.H. Sun, G.A. Tai, S.P. Lau, F. Yan, ACS Nano 6 (2012) 810–818.
[9] Z.C. He, C.M. Zhong, S.J. Su, M. Xu, H.B. Wu, Y. Cao, Nature Photonics 6 (2012) 591–595.
[10] C. Goh, S.R. Scully, M.D. McGehee, Journal of Applied Physics 101 (2007) 114503–114514.
[11] S.D. Oosterhout, M.M. Wienk, S.S.V. Bavel, R. Thiedmann, L.J.A. Koster, J. Gilot, J. Loo, V. Schmidt, R.A.J. Janssen, Nature Materials 8 (2009) 818–824.
[12] S.J. Wu, Q.D. Tai, F. Yan, Journal of Physical Chemistry C 114 (2010) 6197–6200.
[13] Q.D. Tai, X.Z. Zhao, F. Yan, Journal of Materials Chemistry 20 (2010) 7366–7371.
[14] Y.Y. Lin, T.H. Chu, S.S. Li, C.H. Chuang, C.H. Chang, W.F. Su, C.P. Chang, M.W. Chu, C.W. Chen, Journal of the American Chemical Society 131 (2009) 3644–3649.
[15] K.M. Noone, N.C. Anderson, N.E. Horwitz, A.M. Munro, Abhishek P. Kulkarni, D.S. Ginger, ACS Nano 3 (2009) 1345–1352.
[16] Wendy U. Huynh, Janke J. Dittmer, A. Paul Alivisatos, Science 295 (2002) 2425–2427.
[17] B. Sun, E. Marx, N.C. Greenham, Nano Letters 3 (2003) 961–963.
[18] M. Schierhorn, S.W. Boettcher, J.H. Peet, E. Matioli, G.C. Bazan, G.D. Stucky, M. Moskovits, ACS Nano 4 (2010) 6132–6136.
[19] J. Boucle, S. Chyla, M.S.P. Shaffer, J.R. Durrant, D.D.C. Bradley, J. Nelson, Advanced Functional Materials 18 (2008) 622–633.
[20] H.S. Shim, S.I. Na, S.H. Nam, H.J. Ahn, H.J. Kim, D.Y. Kim, W.B. Kim, Applied Physics Letters 92 (2008) 183107–183109.
[21] Youngjo Tak, Suk Joon Hong, Jae Sung Lee, Kijung Yong, Journal of Materials Chemistry 19 (2009) 5945–5951.
[22] R. Zhu, C.Y. Jiang, B. Liu, S. Ramakrishna, Advanced Materials 21 (2009) 994–1000.
[23] D. Li, Y.L. Wang, Y.N. Xia, Advanced Materials 16 (2004) 2062–2066.
[24] H. Tang, F. Yan, Q.D. Tai, H.L.W. Chan, Biosensors and Bioelectronics 25 (2010) 1646–1651.
[25] D.R. Baker, P.V. Kamat, Advanced Functional Materials 19 (2009) 805–811.
[26] R.S. Mane, M.Y. Yoon, H. Chung, S.H. Han, Solar Energy 81 (2007) 290–293.
[27] X.F. Gao, W.T. Sun, Z.D. Hu, G. Ai, Y.L. Zhang, S. Feng, F. Li, L.M. Peng, Journal of Physical Chemistry C 113 (2009) 20481–20485.
[28] Y. Kang, D. Kim, Solar Energy Materials and Solar Cells 90 (2006) 166–174.
[29] E.D. Spoerke, M.T. Lloyd, E.M. Mccready, D.C Olson, Y.J. Lee, J.W.P. Hsu, Applied Physics Letters 95 (2009) 213506–213508.
[30] Y.Z. Hao, Y.H. Cao, B. Sun, Y.P. Li, Y.H. Zhang, D.S. Xu, Solar Energy Materials and Solar Cells 101 (2012) 107–113.
[31] S. Chun, K.S. Han, J.S. Lee, H.J. Lim, H. Lee, D. Kim, Current Applied Physics 10 (2010) S196–S200.
[32] Z.H. Sun, J.H. Li, C.M. Liu, S.H. Yang, F. Yan, Advanced Materials 23 (2011) 3648–3652.